Thermal properties of Ti-doped Cu-Zn soft ferrites used as thermally actuated material for magnetizing superconductors

P Stachowiak,[1] J Mucha,[1] D Szewczyk,[1] Y Zhai,[2] C H Hsu,[2] T A Coombs,[2] J F Fagnard,[3] M P Philippe[3] and P Vanderbemden[3*]

[1] W Trzebiatowski Institute for Low Temperature and Structure Research, Polish Academy of Sciences, PO Box 1410, 50-950 Wroclaw 2, Poland

[2] EPEC Superconductivity group, Electrical Engineering Department, Cambridge University, Cambridge CB3 0FA, United Kingdom

[3] University of Liège, SUPRATECS, Department of Electrical Engineering & Computer Science (B28), Quartier Polytech, Sart-Tilman, B-4000 Liège, Belgium

* (corresponding author), e-mail: Philippe.Vanderbemden@ulg.ac.be

Abstract. A great majority of widely used ferrite ceramics exhibit a relatively high temperature of order-disorder phase transition in their magnetic subsystem. For applications related to the magnetization process of superconductors, however, a low value of T_c is required. Here we report and analyze in detail the thermal properties of bulk Ti-doped Cu-Zn ferrite ceramics $Cu_{0.3}Zn_{0.7}Ti_{0.04}Fe_{1.96}O_4$ and $Mg_{0.15}Cu_{0.15}Zn_{0.7}Ti_{0.04}Fe_{1.96}O_4$. They are characterized by a Curie temperature in the range 120-170 K and a maximum DC magnetic susceptibility exceeding 20 for the $Cu_{0.3}Zn_{0.7}Ti_{0.04}Fe_{1.96}O_4$ material. The temperature dependence of both the specific heat C_p and of the thermal conductivity κ, determined between 2 and 300 K, are found not to exhibit any peculiar feature at the magnetic transition temperature. The low-temperature dependence of both κ and the mean free path of phonons suggests a mesoscopic fractal structure of the grains. From the measured data, the characteristics of thermally actuated waves are estimated. The low magnetic phase transition temperature and suitable thermal parameters make the investigated ferrite ceramics applicable as magnetic wave producers in devices designed for magnetization of high-temperature superconductors.

PACS: 75.50.Gg, 72.20.-I, 74.25.N-

1

1. Introduction

Due to the combination of excellent magnetic properties at high frequency and low price, ferrite materials have become essential materials in a wide range of electrical engineering applications including chip components, filters, telecommunication systems, sensors [1-5] and extending to biomedical applications and energy storage [6-8]. This present work deals with ferrites to be inserted in an innovative low-temperature application related to the magnetization of type-II superconductors used as permanent magnets [9,10]. Unlike a classical ferromagnet where the magnetization is limited physically by the alignment of all microscopic magnetic moments, the remnant magnetization of a type-II irreversible superconductor is generated by macroscopic (resistanceless) supercurrent current loops [11,12]. When prepared in bulk form, e.g. monolithic disks of a few centimeters in diameter [13-16], superconductors are able to trap magnetic flux densities exceeding 3 teslas [11, 17-19], which opens up new horizons in terms of applications [20-22]. One of the main issues, however, is that these superconducting materials need to be magnetized before their use. In addition to the well-established magnetization techniques, - namely, zero field cooling (ZFC), field cooling (FC) and pulse field magnetization (PFM) [23] -, there is a growing interest in applying the so-called "flux pump" technology [24] to the magnetization of bulk superconductors [25,26]. Flux pumping involves creating a travelling magnetic field wave that guides magnetic flux lines toward the center of the superconducting element. The technique can be applied to films, bulk samples or coils [27]. The travelling wave can be produced by a moving magnet [26], a three-phase coil system [28] or by making use of the so-called "Thermally Actuated Magnetization" (TAM) [9,10,25]. In the latter, the bulk superconductor is placed below a magnetic disk exhibiting a clear phase transition at some (Curie) temperature T_c, as shown schematically in figure 1(a). Periodic heating and cooling of the magnetic material at its periphery generates a thermal wave that travels radially. If the two extrema of the temperature oscillations are respectively below and above T_c, the corresponding periodic changes of permeability of the magnetic material in a DC background field results in a travelling magnetic field wave. The application of travelling wave to superconducting bulks or films gives rise to vortex migration and to several phenomena of interest for the understanding of physics of type-II superconductors [29].

The key element of a thermally actuated magnetization system is the magnetic material in which the wave is produced. It should ideally exhibit a sharp change of permeability at the ordered-disordered phase transition temperature and this temperature should be between room temperature and the operating temperature of the superconductor (e.g. 77 K or lower). With a critical temperature of 292 K [30,31], gadolinium (Gd) has been shown to be an efficient thermal material [25]. One of the disadvantages is that the magnetic actuation needs to be performed around room temperature, while the superconductor is kept at its operating (cryogenic) temperature, thereby requiring efficient thermal insulation between both. In order to scale up the system for various superconductor sizes at reasonable cost as well as to improve its performances, several magnetic materials with lower transition temperatures were
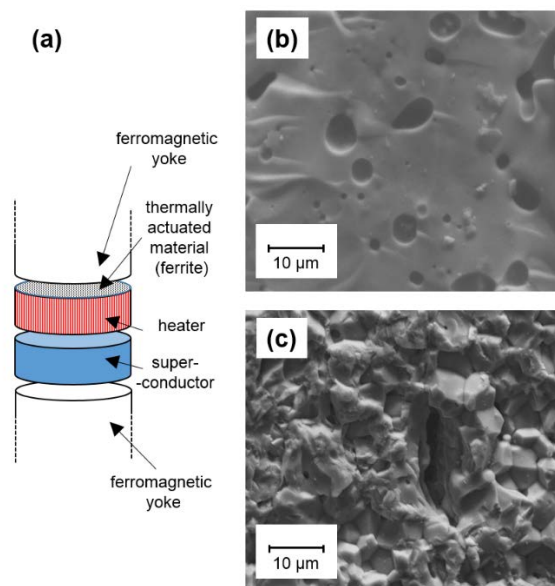
Figure 1. (a) Schematic diagram of the thermally actuated magnetization system: the bulk superconductor is placed below a ferrite material heated repeatedly by an electric heater placed along its lateral surface. A ferromagnetic yoke is used to close the magnetic circuit. (b) SEM image of the surface of the investigated $Cu_{0.3}Zn_{0.7}Ti_{0.04}Fe_{1.96}O_4$ sample. (c) SEM image of the surface of the investigated $Mg_{0.15}Cu_{0.15}Zn_{0.7}Ti_{0.04}Fe_{1.96}O_4$ sample.

investigated: these including manganites [32] or ferrites [33]. Among the several chemical compositions investigated in Ti-doped Ni-Zn and Cu-Zn ferrites, the most promising results were obtained from $Cu_{0.3}Zn_{0.7}Ti_{0.04}Fe_{1.96}O_4$ and $Mg_{0.15}Cu_{0.15}Zn_{0.7}Ti_{0.04}Fe_{1.96}O_4$ stoichiometry [9,10]. Their critical temperature is much lower than that of commercial ferrites, while their magnetic properties remain weakly affected. In addition to their magnetic properties and the implications when ferro- or ferrimagnets and superconductors are brought together [34,35], thermal properties of these materials are likely to play an important role in the magneto-thermal actuation process. The aim of the present work is to investigate in detail the physics of the thermal properties of these ferrite ceramics and to draw conclusions as to the implications for the characteristics of thermally actuated waves when used for the magnetization of bulk superconductors.

2. Experiment

Ti-doped Cu-Zn ferrite ceramics were prepared using the solid-state reaction method described in details in references [9,10]. High-purity powders of CuO, ZnO, TiO_2 and $FeC_2O_4 \cdot 2\,H_2O$ were mixed homogeneously and progressively heated to 1200°C with an intermediate grinding. This method can be used routinely to obtain resulting ferrite pellets are disks of 22 mm in diameter and 11 mm in height. The stoichiometry of the two compounds studied in this work is $Cu_{0.3}Zn_{0.7}Ti_{0.04}Fe_{1.96}O_4$ and
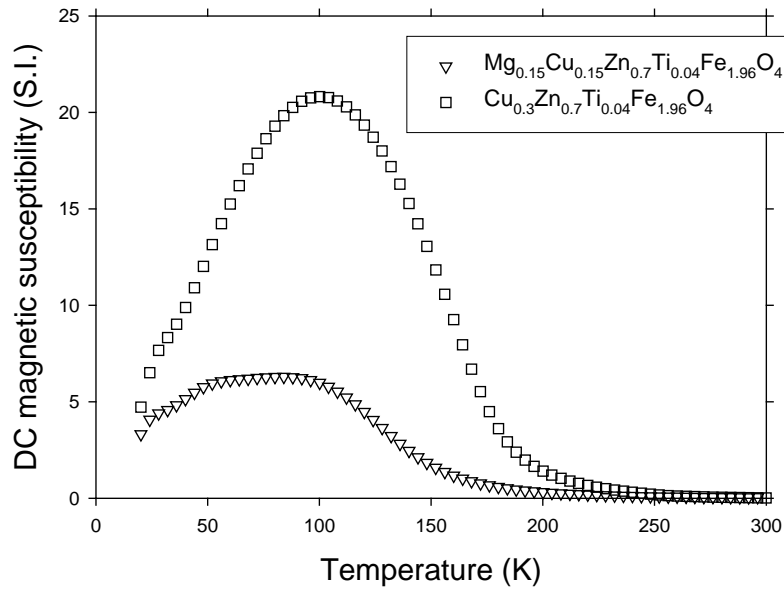
$Mg_{0.15}Cu_{0.15}Zn_{0.7}Ti_{0.04}Fe_{1.96}O_4$. X-ray diffraction (XRD) and energy dispersive X-ray (EDX) analyses confirm that no secondary phase was present in the samples [9]. A typical scanning electron microscope (SEM) image of the cross-section of both ferrite samples is shown in figure 1(b) and 1(c). Their microstructure is typical of well-sintered materials. For $Mg_{0.15}Cu_{0.15}Zn_{0.7}Ti_{0.04}Fe_{1.96}O_4$, individual grains can be distinguished easily, with an average size of about 1-5 micrometers. The structure of a grain itself was reported in a previous work [36]. The $Cu_{0.3}Zn_{0.7}Ti_{0.04}Fe_{1.96}O_4$ and $Mg_{0.15}Cu_{0.15}Zn_{0.7}Ti_{0.04}Fe_{1.96}O_4$ form a cubic crystal structure with 32 oxygen atoms in a unit cell and the cell parameter amounting to ~ 8Å. The typical electrical resistivity of the investigated ferrite materials lies in the range 10^4-10^5 Ωm.

Magnetic measurements as a function of temperature were performed in a Quantum Design Physical Property Measurement System (PPMS). Small rectangular prisms of typical dimensions $0.65 \times 0.65 \times 7$ mm were carefully excised from the main ferrite pellet using a wire saw. In each measurement, the magnetic field was always applied along the long axis of the sample. The large aspect ratio (length/average diameter) ensured that the demagnetization factor D is small enough, so that the measured magnetic susceptibility is not bounded by a temperature-independent limit given by $1/D$ [37,38]. Unlike fluxmetric methods involving a search coil wound around the central part of the sample [39], the magnetic susceptibility of the ferrite (volume V) is determined through measurement of the magnetic moment m, from which the magnetization $M = m/V$ is deduced [38]. The intrinsic magnetic susceptibility χ_{int} is then determined from the measured (apparent) susceptibility $\chi_{ext} = M/H_a$, where H_a is the uniform applied field, using magnetometric demagnetization factors for rectangular prisms [40-42]. In order to take into account of the magnetic susceptibility dependence of the demagnetization factor, the iterative method suggested in ref. [42] was followed. The corresponding magnetometric demagnetization factors were found to be less than 0.042.

Specific heat and thermal conductivity measurements were also carried out using Quantum Design Physical Properties Measurement System (PPMS). The specific heat was measured with a dynamic method while the thermal conductivity coefficient dependence on temperature of the investigated materials was determined by steady state heat flow method. The thermal properties were measured in the temperature range 2-300 K.

3. Results and discussion

In this section we present and discuss the magnetic properties and the thermal properties (specific heat, thermal conductivity and thermal diffusivity) of the ferrite compounds investigated. It should be noted here that several physical properties of ceramics such as their thermal, mechanical electric or magnetic properties are closely related to the structure and texture transitions which take place during the process of long-term sintering of the materials. The change of dimensions of the grains is an effect of diffusive
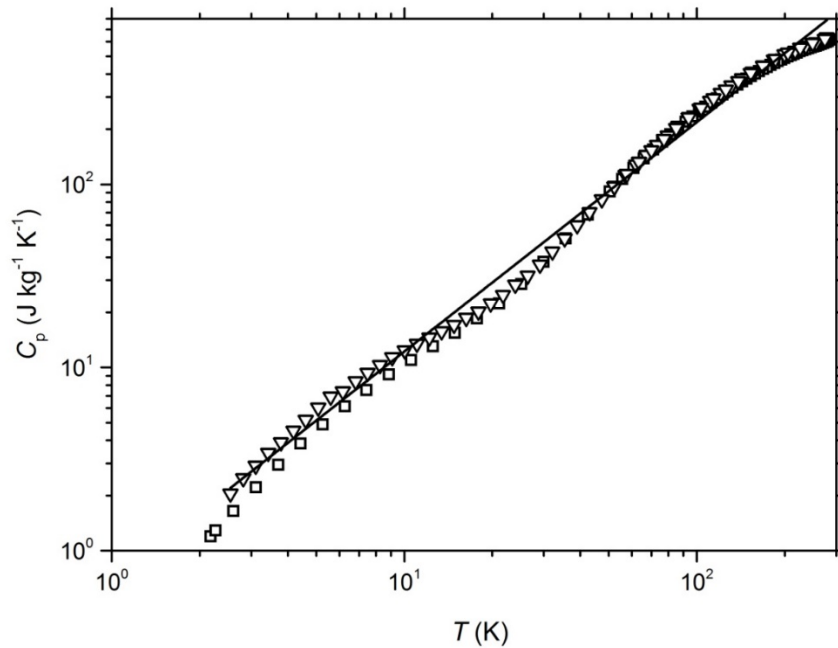
Figure 2. Temperature dependence of the DC magnetic susceptibility for the $Cu_{0.3}Zn_{0.7}Ti_{0.04}Fe_{1.96}O_4$ (squares) and $Mg_{0.15}Cu_{0.15}Zn_{0.7}Ti_{0.04}Fe_{1.96}O_4$ ferrites (triangles). Data (corrected for demagnetizing effects) are measured for an applied field of 10 mT in Zero-Field Cooled (ZFC) procedure.

transfer of mass between the grains remaining in mechanical contact. The process results in an increase of volume of some grains at the expense of the neighbouring ones. This leads to a decrease in size, and sometimes a complete disappearance of the grain and the formation of amorphous structures filling the in-between grain volume [43]. All of the processes and therefore the features of the structure strongly influence the specific heat and the thermal transport processes in ceramics. For this reason, the interpretation of the thermal properties experimental results is rather difficult and is usually limited to the simple classical models.

3.1. DC magnetic susceptibility

Figure 2 shows the temperature dependence of magnetic DC susceptibility χ of the two ferrite compounds measured for an applied field of 10 mT in Zero-Field Cooled (ZFC) procedure. Both materials exhibit an ordered – disordered phase transition at a temperature T_c that can be determined from the inflection point of the $\chi(T)$ curves. This procedure leads to $T_c \approx 160$ K. for $Cu_{0.3}Zn_{0.7}Ti_{0.04}Fe_{1.96}O_4$ and $T_c \approx 125$ K for $Mg_{0.15}Cu_{0.15}Zn_{0.7}Ti_{0.04}Fe_{1.96}O_4$. The role of the Mg dopant for the Cu-Zn ferrite appears clearly since the transition temperature is reduced by ~ 35 K. This decrease is beneficial for driving the operating temperature of the thermally actuated material closer to operating temperature of the superconductors of interest, e.g. 77 K for the $YBa_2Cu_3O_7$ compound [12-15].

Figure 3. Temperature dependence of specific heat of $Cu_{0.3}Zn_{0.7}Ti_{0.04}Fe_{1.96}O_4$ (squares) and $Mg_{0.15}Cu_{0.15}Zn_{0.7}Ti_{0.04}Fe_{1.96}O_4$ (triangles) ferrites. The solid line is a plot of the function $C_p = 0.68T^{1.25}$ [J kg^{-1} K^{-1}], which approximates the $Cu_{0.3}Zn_{0.7}Ti_{0.04}Fe_{1.96}O_4$ sample specific heat data. An absence of any noticeable singularity at the temperatures of the magnetic phase transition, 160 K and 125 K for $Cu_{0.3}Zn_{0.7}Ti_{0.04}Fe_{1.96}O_4$ and $Mg_{0.15}Cu_{0.15}Zn_{0.7}Ti_{0.04}Fe_{1.96}O_4$ respectively, testifies for negligible contribution of thermal excitations in the magnetic subsystem of both ferrites.

The change in magnetic susceptibility $\Delta\chi$, however, that can be expected by sweeping the ferrite temperature by 10 K below and above T_c is found to be much smaller for $Mg_{0.15}Cu_{0.15}Zn_{0.7}Ti_{0.04}Fe_{1.96}O_4$ ($\Delta\chi = 2.03$) than for $Cu_{0.3}Zn_{0.7}Ti_{0.04}Fe_{1.96}O_4$ ($\Delta\chi = 6.37$). This feature can be attributed to both the higher magnetic moment and narrower transition for the $Cu_{0.3}Zn_{0.7}Ti_{0.04}Fe_{1.96}O_4$ compound. The latter is to be preferred, therefore, for thermal actuation. The maximum intrinsic susceptibility of this compound, at $T = 101$ K, was found to be $\chi_{int} = 20.8$ (cf. figure 2) and is comparable in magnitude to the values reported for gadolinium [30]. In the present case, we emphasize that the maximum external magnetic susceptibility ($\chi_{ext} = 13.9$) is significantly smaller than the demagnetizing-limited value estimated at this temperature ($1/D \approx 41.7$, where D is the magnetometric demagnetization factor). This gives confidence that the numerical values displayed in figure 2 are not bounded by geometric effects, as can be the case when small single crystals with low aspect ratio are studied [44], and is further confirmed by the clear temperature dependence observed in figure 2.
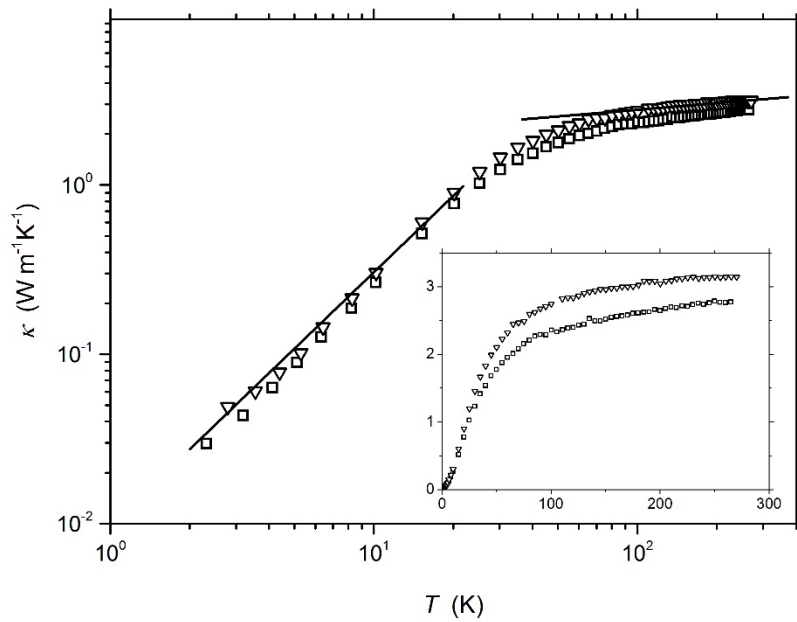
Figure 4. Temperature dependence of thermal conductivity coefficient of $Cu_{0.3}Zn_{0.7}Ti_{0.04}Fe_{1.96}O_4$ (squares) and $Mg_{0.15}Cu_{0.15}Zn_{0.7}Ti_{0.04}Fe_{1.96}O_4$ (triangles) ferrites. The solid lines show the results of fitting of a power function to the data obtained for $Mg_{0.15}Cu_{0.15}Zn_{0.7}Ti_{0.04}Fe_{1.96}O_4$ sample, for the temperatures below 20 K and above 100 K. The slope of the lines is 1.6 and 0.13, respectively. The inset shows the same experimental data in double-linear coordinates.

3.2. Specific heat

The results of the measurements of the specific heat C_p of the samples of both investigated ferrites carried out in the temperature range 2 – 270 K are shown in figure 3. Unlike magnetic data, the specific heats of the two compounds are found to be almost identical at the investigated temperatures. The temperature dependence can be roughly approximated with $C_p \sim T^{1.25}$. Such a dependence indicates that in the investigated ceramics the excitations of phonons such as those described by the Debye and Einstein models, do not contribute significantly to the specific heat. Also, in the dependence, there is no evidence of change of magnetic ordering at the transition temperature ($T_c = 125$ K and 160 K), unlike the behaviour observed for gadolinium [44] or other Zn-Mn or Zn-Ni ferrites [45]. This seems to indicate that the magnetic component of the specific heat may be negligibly small.

3.3. Thermal conductivity

Figure 4 shows the measurements of the thermal conductivity coefficient κ dependence on temperature for $Cu_{0.3}Zn_{0.7}Ti_{0.04}Fe_{1.96}O_4$ and $Mg_{0.15}Cu_{0.15}Zn_{0.7}Ti_{0.04}Fe_{1.96}O_4$ ceramics. The main plot of the data is

shown in logarithmic coordinates while the same set of data is depicted in linear coordinates in the inset. In the temperature range of 2 – 300 K the coefficient changes monotonically from 0.2 $Wm^{-1}K^{-1}$ at the lowest temperature to approximately 2.5 – 3 $Wm^{-1}K^{-1}$ at the highest investigated temperature. These high-temperature values are close to the majority of other ferrite materials [46]. Initially, up to ~ 30 K the thermal conductivity changes ~ $T^{1.6}$. Such low temperature dependence resembles the dependence of thermal conductivity coefficient on temperature of solids featuring a fractal structure. It was shown [47,48] that for these solids $\kappa \sim T^{n}$, with n = d+1-2d/E, where E and d denote the structural fractal and the spectral dimension, respectively, for a mesoscopic fractal structure the value of the exponent n will be close to the one found in our experiment [49].

At the temperatures above 30 K the thermal conductivity coefficient of $Mg_{0.15}Cu_{0.15}Zn_{0.7}Ti_{0.04}Fe_{1.96}O_4$ shows a slightly higher value than that found for $Cu_{0.3}Zn_{0.7}Ti_{0.04}Fe_{1.96}O_4$. In the temperature range 100 – 300 K the difference remains constant and amounts to ~ 0.4 $Wm^{-1}K^{-1}$. This difference is most likely related to the difference of masses of Mg and Cu ions. In addition, no anomaly is found at the transition temperature, unlike the behaviour observed e.g. for the ferrite material Mn_3O_4 [50].

Both $Mg_{0.15}Cu_{0.15}Zn_{0.7}Ti_{0.04}Fe_{1.96}O_4$ and $Cu_{0.3}Zn_{0.7}Ti_{0.04}Fe_{1.96}O_4$ are characterized by high electrical resistivity values [36], as is the case for other undoped Cu-Zn ferrites [51]. Additionally, from specific heat measurements there is no evidence of meaningful energy of magnon excitations. It can be assumed, therefore, that the heat transport in the investigated ceramics is realized mostly by phonons [52]. In such a situation, the thermal conductivity coefficient can be written in terms of phonon mean path $\ell(T)$ by the kinetic equation:

$$\kappa(T)=1/3 \vartheta C_{vol}(T)\ell(T), \qquad\qquad (1)$$

where $C_{vol}(T)$ is the volumetric specific heat and ϑ is the phonon group velocity averaged over longitudinal and transverse phonons. The phonon mean free path (being a value averaged over phonon frequencies and polarizations) dependence on temperature found from the above equation for $Mg_{0.15}Cu_{0.15}Zn_{0.7}Ti_{0.04}Fe_{1.96}O_4$ and $Cu_{0.3}Zn_{0.7}Ti_{0.04}Fe_{1.96}O_4$ is shown in figure 5. For the calculations the data obtained in thermal conductivity and specific heat experiments were used ($C_{vol} = \rho C_p$, where ρ = 4600 kgm^{-3} is the density of the ferrite material). For the velocity of phonons an arbitrary taken value of a typical sound velocity in ceramics ϑ = 4000 ms^{-1} [53] was applied. From the data plotted in figure 5 one can notice that the phonon mean free path in the whole investigated temperature range is at least two orders of magnitude smaller than the linear dimensions of crystallites forming the ferrite. Grain boundary scattering, therefore, is not the most important phonon scattering mechanism even at the
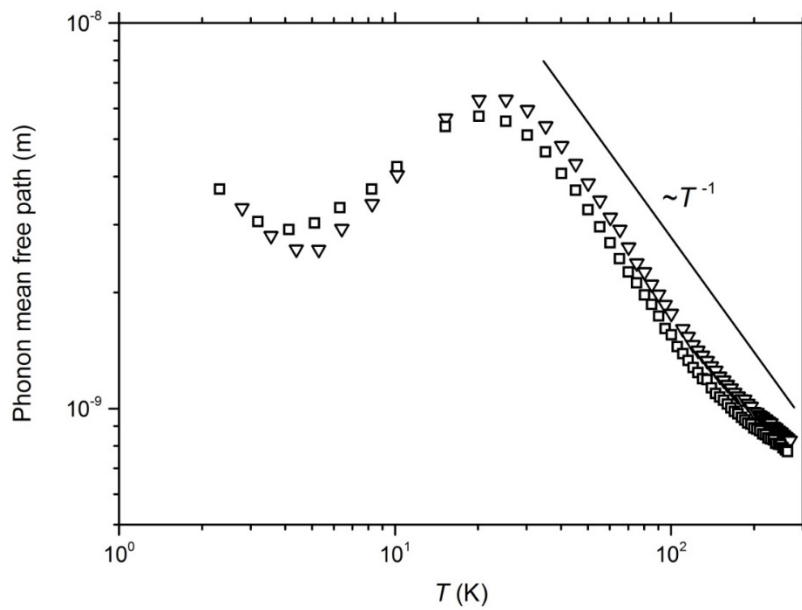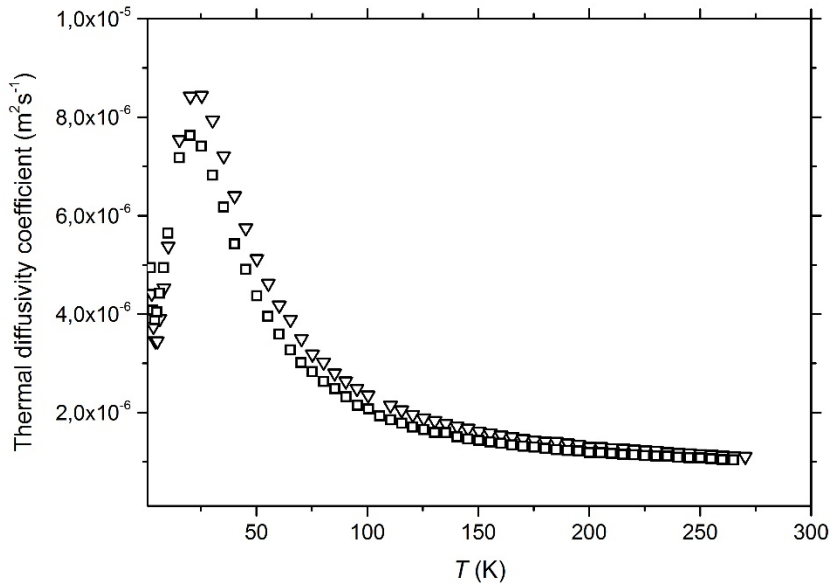
Figure 5. Temperature dependence of the phonon mean free path in the investigated $Cu_{0.3}Zn_{0.7}Ti_{0.04}Fe_{1.96}O_4$ (squares) and $Mg_{0.15}Cu_{0.15}Zn_{0.7}Ti_{0.04}Fe_{1.96}O_4$ (triangles) ferrites. The high temperature part of the dependence is well approximated by a function $\sim T^{-1}$, which is shown schematically with a solid line. Such temperature dependence of the phonon mean free path found for both samples may be considered as an evidence of domination of U-processes in phonon scattering processes in this temperature region.

lowest investigated temperatures. Such a short low-temperature phonon mean free path, again seems to confirm the fractal structure of the grain of the investigated ferrites [49]. In the temperature range 20 – 180 K the dependence can be roughly approximated by T^{-1}. This may be considered as evidence of dominating phonon-phonon interactions in U-processes in these temperatures [54].

3.4. Thermal diffusivity

The value of the thermal diffusivity is of great importance in case of functional materials which are designed for generating travelling waves. The thermal diffusivity coefficient is given by the following expression

Figure 6. Temperature dependence of the thermal diffusivity coefficient for the investigated Cu$_{0.3}$Zn$_{0.7}$Ti$_{0.04}$Fe$_{1.96}$O$_4$ (squares) and Mg$_{0.15}$Cu$_{0.15}$Zn$_{0.7}$Ti$_{0.04}$Fe$_{1.96}$O$_4$ (triangles) ferrites.

$$\alpha(T) = \kappa(T)/\big(\rho C_p(T)\big). \tag{2}$$

It can be seen clearly that the thermal diffusivity coefficient depends linearly on the mean free path of the phonons. The dependence of the coefficient on temperature, found for the investigated samples, was calculated with the above equation. Results are shown in figure 6. The thermal diffusivity over the whole investigated temperature range is a little higher for Mg$_{0.15}$Cu$_{0.15}$Zn$_{0.7}$Ti$_{0.04}$Fe$_{1.96}$O$_4$ than for Cu$_{0.3}$Zn$_{0.7}$Ti$_{0.04}$Fe$_{1.96}$O$_4$ ferrite and both are comparable to the group of ceramics showing rather low thermal diffusivity coefficient [46].

The thermal diffusivity values determined above can be used to estimate the characteristics of thermally actuated waves in the ferrite material. In the targeted application, the ferrite disk is heated repeatedly by a heater placed around its periphery, as shown schematically in figure 1(a). In the simplest analysis, we can assume the cylinder to be infinite. Due to the axisymmetric geometry, a 1D model where temperature is only function of radial distance and time, i.e. $T(r,t)$, can be used. If the parabolic heat diffusion equation is assumed to hold, the temperature distribution within an infinite plain cylindrical sample (radius a) subjected to the steady-periodic surface temperature $T(a,t) = T_0 + Ae^{i\omega t}$ with $\omega = 2\pi/\tau_0$ is given by [55]

$$T(r,t) = T_0 + A \frac{I_0(kr)}{I_0(ka)} e^{i\omega t} \tag{3}$$

where I_0 is the modified Bessel function of the first kind zero order and $k^2 = \frac{i\omega}{\alpha}$, where α is the thermal diffusivity. Note that this equation is only valid if the period of the applied excitation, τ_0, is much larger than the intrinsic thermal relaxation time (τ) of the material, otherwise more sophisticated models [56] and the hyperbolic form of the heat equation [57] should be used. In such a case one has $k^2 = \frac{(i\omega - \tau\omega^2)}{\alpha}$ [55]. The order of magnitude of the thermal relaxation time estimated for metals, and semiconductors ranges between 10^{-12} s and 10^{-6} s [58]. Even if τ is probably larger for ceramics and at cryogenic temperature, its effect is likely negligible since the temperature excitation period τ_0, is of the order of 1 second or more. From the formulas above, the thermal diffusion length μ is given by

$$\mu = \sqrt{\frac{2\alpha}{\omega}}. \tag{4}$$

Good working conditions require the thermal diffusion length to be of the order of the sample radius. Due to their thermal conductivity being significantly lower than gadolinium around its Curie temperature [59, 60], the thermal diffusivity of the ferrite compounds around their T_c is approx. 2.6 times smaller than that of gadolinium around its transition temperature. In order to activate the entire volume of the sample, therefore, the period of the temperature excitation for ferrites has to be increased accordingly. In practice, the real system involving a ferrite sample of finite height is more complex that a simple radial heat flow and numerical magneto-thermal simulations should be used [61]. The thermal property values determined in this work are therefore of definite interest for the finite-element modelling of the magnetization of superconductors using thermally actuated materials.

4. Conclusion

The measurements of magnetic susceptibility, specific heat and thermal conductivity coefficient dependencies on temperature of $Mg_{0.15}Cu_{0.15}Zn_{0.7}Ti_{0.04}Fe_{1.96}O_4$ and $Cu_{0.3}Zn_{0.7}Ti_{0.04}Fe_{1.96}O_4$ ferrite ceramics were carried out in the temperature range 2 – 300 K. The investigated ferrites are characterized by a magnetic order-disorder phase transition in the temperature range 120 – 170 K. Neither specific heat, nor thermal conductivity, data show evidence of noticeable contribution of magnetic subsystem thermal excitation to the whole thermal energy of the investigated ferrites. This fact, along with high electrical resistivity of the ceramics, testifies to the dominant phononic character of thermal excitation and thermal transport in the ceramics. From the thermal parameters obtained in the experiment, phonon mean free path and thermal diffusivity dependencies on temperature were inferred. The low-temperature

dependence of the thermal conductivity coefficient on temperature and the value of the phonon mean free path at low temperatures suggest a mesoscopic fractal structure of the grains of the investigated ferrites. According to a theoretical estimation of the properties of thermal waves in cylindrical geometry, the magnetic and thermal characteristics of $Mg_{0.15}Cu_{0.15}Zn_{0.7}Ti_{0.04}Fe_{1.96}O_4$ and $Cu_{0.3}Zn_{0.7}Ti_{0.04}Fe_{1.96}O_4$ ferrite ceramics, which were specified in the current paper, make them good candidates for magnetic wave producers in devices for magnetization of high-temperature superconducting ceramics.

Acknowledgments

References

[1]   Sugimoto M 1999 *J. Am. Ceram. Soc.* **82** 269

[2]   Taniguchi K, Abe N, Ohtani S, Umetsu H and Arima T 2008 *Appl. Phys. Express* **1** 031301

[3]   Koutzarova T, Kolev S, Nedkov I, Krezhov K, Kovacheva D, Blagoev B, Ghelev C, Henrist C, Cloots R and Zaleski A 2012 *J. Supercond. Nov. Magn.* **25** 2631

[4]   Ming Li *et al* 2013 *J. Phys. D: Appl. Phys.* **46** 275001

[5]   Sanada M, Inoue Y and Morimoto S 2014 *Electrical Engineering in Japan* **1** 187

[6]   Sanpo N, Wen C, Berndt C C and Wang J 2015 In : *Advanced Functional Materials* (eds A. Tiwari and L. Uzun), John Wiley & Sons, Inc., Hoboken, NJ, USA 183

[7]   Belous A G, Solovyova E D, Solopan S O, Yelenich O V, Bubnovskaya L N and Osinsky S P 2015 *Solid State Phenom.* **230** 95

[8]   Xia T, Xu X, Wang J, Xu C, Meng F, Shi Z, Lian J and Bassat J M 2015 *Electrochim. Acta* 160 114

[9]   Hsu C H, Yan Y, Hadeler O, Vertuyen B, Granados X and Coombs T A 2012 *IEEE Trans. Appl. Supercond.* **22** 7800404

[10]   Zhai Y, Hsu C H, Spaven F, Zhang M, Wang W and Coombs T A 2013 *IEEE Trans. Appl. Supercond.* **23** 7800104

[11]   Tomita M and Murakami M 2003 Nature **421** 517

[12]   Vanderbemden P, Hong Z, Coombs T A, Denis S, Ausloos M, Schwartz J, Rutel I B, Hari Babu N, Cardwell D A and Campbell A M 2007 *Phys. Rev. B* **75** 174515

[13]   Devendra Kumar N, Shi Y, Zhai W, Dennis A R, Durrell J H and Cardwell D A 2015 *Cryst. Growth Des.* **15** 1472

[14]   Teshima H, Morita M, Arayashiki T, Naito T and Fujishiro H 2013 *Phys. Procedia* **45** 61

[15] Chaud X, Kenfaui D, Louradour E and Noudem J G 2012 *IEEE Trans. Appl. Supercond.* **22** 6800304

[16] Doyle R A, Bradley A D, Lo W, Cardwell D A, Campbell A M, Vanderbemden P and Cloots R 1998 *Appl. Phys. Lett.* **73** 117

[17] Nariki S, Sakai N and Murakami M 2005 *Supercond. Sci. Technol.* **18** S126

[18] Sugino S, Yamamoto A, Shimoyama J and Kishio K 2015 *Supercond. Sci. Technol.* **28** 055016

[19] Durrell J H *et al* 2014 *Supercond. Sci. Technol.* **27** 082001

[20] Masson P J, Breschi M, Tixador P and Luongo C A 2007 *IEEE Trans. Appl. Supercond.* **17** 1533

[21] Werfel F N, Floegel-Delor U, Rothfeld R, Riedel T, Goebel B, Wippich D and Schirrmeister P 2012 *Supercond. Sci. Technol.* **25** 014007

[22] Zhou D, Izumi M, Miki M, Felder B, Ida T and Kitano M 2012 *Supercond. Sci. Technol.* **25** 103001

[23] Fujishiro H, Tateiwa T, Fujiwara A, Oka T and Hayashi H 2006 *Physica C* **445-448** 334

[24] Van Beelen H , Arnold A J P T, Sypkens H A, Van Braam Houckgeest J P, De Bruyn Ouboter R, Beenakker J J M and Taconis K W 1965 *Physica* **31** 413

[25] Coombs T A, Hong Z, Zhu X and Krabbes G 2008 *Supercond. Sci. Technol.* **21** 034001

[26] Davey K R, Weinstein R, Parks D and Sawh R 2011 *IEEE Trans. Magn.* **47** 1090

[27] Yoondo C, Itsuya M, Hoshino T and Nakamura T 2004 *IEEE Trans. Appl. Supercond.* **14** 1723

[28] Wang W and Coombs T A 2013 *J. Appl. Phys.* **113** 213906

[29] Wang W, Spaven F, Zhang M, Baghdadi M and Coombs T A 2014 *Appl. Phys. Lett.* **104** 032602

[30] Coey J M D, Skumryev V and Gallagher K 1999 *Nature* **401** 35

[31] Elliott J F, Legvold S and Spedding F H 1953 *Phys. Rev.* **91** 28

[32] Vertruyen B, Rulmont A, Cloots R, Ausloos M, Dorbolo S and Vanderbemden P 2002 *Materials Letters* **57** 598

[33] Murakami K 1965 *IEEE Trans. Magn.* **1** 96

[34] Philippe M P, Fagnard J F, Kirsch S, Xu Z, Dennis A R, Shi Y H, Cardwell D A, Vanderheyden B and Vanderbemden P 2014 *Physica C* **502** 20

[35] Gömöry F, Solovyov M, Šouc J, Navau C, Prat-Camps J and Sanchez A 2012 *Science* **335** 1466

[36] Hsu C H, PhD Thesis, Department of Engineering, University of Cambridge, July 2013

[37] Fiorillo F 2010 *Metrologia* **47** S114

[38] Vanderbemden P, Vertruyen B, Rulmont A, Cloots R, Dhalenne G and Ausloos M 2003 *Phys. Rev. B* **68** 224418

[39] Vanderbemden P 1998 *Cryogenics* **38** 839

[40] Aharoni A 1998 *J. Appl. Phys.* **83** 3432

[41] Chen D X, Pardo E and Sanchez A 2002 *IEEE Trans. Magn.* **38** 1742

[42] Chen D X, Pardo E and Sanchez A 2005 *IEEE Trans. Magn.* **41** 2077

[43] Jeżowski A, Mucha J, Pązik R and Stręk W 2007 *Appl. Phys. Lett.* **90** 114104

[44] Yu. Dan'kov S, Tishin A M, Pecharsky V K and Gschneidner Jr. K A 1998 *Phys. Rev. B* **57** 3478

[45] Nielsen OV 1969 *Applied Scientific Research* **20** 381

[46] Nelson A T, White J T, Andersson D A, Aguiar J A, McClellan K J, Byler D D, Short M P and Stanek C R 2014 *J. Am. Ceram. Soc.* **97** 1559

[47] de Goer A M, Calemczuk R, Salce B, Bon J, Bonjour E and Maynard R 1989 *Phys. Rev. B* **40** 8327

[48] Maynard R 1990 *Physica A* **168** 469

[49] Lasjaunias J C, Saint-Paul M, Bilusic A, Smontara A, Gradecak S, Tonejc A M, Tonejc A and Kitamura N 2002 *Phys. Rev. B* **66** 014302

[50] Mucha J, Vertruyen B, Misiorek H, Ausloos M, Durczewski K and Vanderbemden P 2009 *J. Appl. Phys.* **105** 063501

[51] Abbas T, Islam M U and Ashraf M 1995 *Mod. Phys. Lett. B* **9** 1419

[52] Berman R, *Thermal Conduction in Solids,* Clarendon Press, Oxford, 1976

[53] Byrne C E and Nagle D C 1997 *Carbon* **35** 267

[54] Ziman J M, *Electrons and Phonons*, Clarendon Press, Oxford, 1979

[55] Zanchini E and Pulvirenti B 1998 *Heat Mass Transfer* **33** 319

[56] Zhang M K 2013 *Int. J. Heat Mass Transfer* **67** 1072

[57] Salazar A 2006 *Eur. J. Phys.* **27** 1349

[58] Ordóñez-Miranda J and Alvarando-Gil J J 2009 *Int. J. Therm. Sci.* **48** 2053

[59] Glorieux C and Thoen J 1994 *Journal de Physique IV* **04(C7)** 271

[60] Jacobsson P and Sundqvist B 1989 *Phys. Rev. B* **40** 9541

[61] Coombs T A 2011 *IEEE Trans. Appl. Supercond.* **21** 3581